

# NLO Event Simulation for Chargino Production at the ILC

Tania Robens <sup>a</sup>

RWTH Aachen - Institut für Theoretische Physik E - 52056 Aachen - Germany

PITHA 07/12, SFB/CPP-07-67

**Abstract.** We present an extension of the Monte Carlo Event Generator **WHIZARD** which includes chargino production at the ILC at NLO. We include photons using both a fixed order and a resummation approach. While the fixed order approach suffers from negative event weights, the resummation method solves this problem and automatically includes leading higher order corrections. We present results for cross sections and event generation for both methods and evaluate the systematic errors due to soft and collinear approximations. In the resummation approach, the residual uncertainty can be brought down to the per-mil level.

This is an updated version of the results presented in [1, 2].

**PACS.** 12.15.Lk Electroweak radiative corrections – 13.66.Hk Production of non-standard model particles in  $ee+$  interactions – 14.80.Ly Supersymmetric partners of known particles

## 1 Introduction

In many GUT models, the masses of charginos tend to be near the lower edge of the superpartner spectrum, and they can be pair-produced at a first-phase ILC with c.m. energy of 500 GeV. The precise measurement of their parameters (masses, mixings, and couplings) is a key for uncovering the fundamental properties of the MSSM [3]. Regarding the experimental precision at the ILC, off-shell kinematics for the signal process, and the reducible and irreducible backgrounds [4] need to be included as well as NLO corrections for chargino production at the ILC which are in the percent regime. We here present the inclusion of the latter.

## 2 Chargino production at LO and NLO

### Fixed order approach

The total fixed-order NLO cross section is given by

$$\sigma_{\text{tot}}(s, m_e^2) = \sigma_{\text{Born}}(s) + \sigma_{\text{v+s}}(s, \Delta E_\gamma, m_e^2) + \sigma_{2 \rightarrow 3}(s, \Delta E_\gamma, m_e^2), \quad (1)$$

where  $s$  is the cm energy,  $m_e$  the electron mass, and  $\Delta E_\gamma$  the soft photon energy cut dividing the photon phase space. The ‘virtual’ contribution  $\sigma_{\text{v}}$  is the interference of the one-loop corrections [5] with the Born term. The collinear and infrared singularities are regulated by  $m_e$  and the photon mass  $\lambda$ , respectively. The dependence on  $\lambda$  is eliminated by adding the soft real

photon contribution  $\sigma_s = f_{\text{soft}} \sigma_{\text{Born}}(s)$  with a universal soft factor  $f_{\text{soft}}(\frac{\Delta E_\gamma}{\lambda})$  [6]. We break the ‘hard’ contribution  $\sigma_{2 \rightarrow 3}(s, \Delta E_\gamma, m_e^2)$ , i.e., the real-radiation process  $e^- e^+ \rightarrow \tilde{\chi}_i^- \tilde{\chi}_j^+ \gamma$ , into a collinear and a non-collinear part, separated at a photon acollinearity angle  $\Delta\theta_\gamma$  relative to the incoming electron or positron. The collinear part is approximated by convoluting the Born cross section with a structure function  $f_h(x; \Delta\theta_\gamma, \frac{m_e^2}{s})$  [7]:

$$\sigma_{\text{h,c}}(\Delta E, \Delta\theta, s) = \int_{\Delta E, 0}^{E_{\text{max}}, \Delta\theta} dx_i d\Gamma_2 f_h(x_i) |\mathcal{M}_b|^2(x_i, s), \quad (2)$$

where  $x_i$  denotes the momentum fraction of the respective incoming beam after photon radiation. The non-collinear part is generated explicitly using exact three particle final state kinematics.

The total fixed order cross section is implemented in the multi-purpose event generator **WHIZARD** [8, 9] using a ‘user-defined’ structure function and an effective matrix element

$$|\mathcal{M}_{\text{eff}}|^2 = (1 + f_s(\Delta E_\gamma, \lambda)) |\mathcal{M}_{\text{born}}|^2 + 2 \text{Re}(\mathcal{M}_{\text{born}} \mathcal{M}_{\text{virt}}^*(\lambda)) \quad (3)$$

which contains the Born part, the soft-photon factor and the Born-1 loop interference term. In the soft-photon region this approach runs into the problem of negative event weights [10]: for some values of  $\theta$ , the  $2 \rightarrow 2$  part of the NLO-corrected squared matrix element is positive definite by itself only if  $\Delta E_\gamma$  is sufficiently large, cf Fig. 1. To still obtain unweighted event samples, an ad-hoc approach is to simply drop events with negative events before proceeding further.

<sup>a</sup> Email: robens@physik.rwth-aachen.de

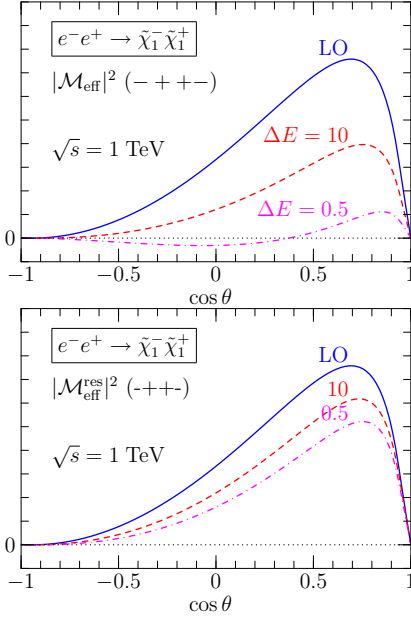


**Fig. 1.**  $\theta$ -dependence of effective squared matrix element ( $\sqrt{s} = 1$  TeV). Upper figure: fixed order effective matrix element; lower figure: effective matrix element with the one-photon ISR part subtracted. Blue/ solid line: Born term; red/ dashed: including virtual and soft contributions for  $\Delta E_\gamma = 10$  GeV; magenta/ dotted: same with  $\Delta E_\gamma = 0.5$  GeV.  $\Delta\theta_\gamma = 1^\circ$ .

### Resummation approach

Negative event weights can be avoided by resumming higher-order initial radiation using an exponentiated structure function  $f_{\text{ISR}}$  [11,12]. In order to avoid double-counting in the combination of the ISR-resummed LO result with the additional NLO contributions [5], we have subtracted from the effective squared matrix element the soft and virtual photonic contributions that have already been accounted for in  $\sigma_{\text{s+v}}$ . This defines

$$|\mathcal{M}_{\text{eff}}^{\text{res}}|^2 = |\mathcal{M}_{\text{eff}}|^2 - 2f_{\text{soft,ISR}} |\mathcal{M}_{\text{Born}}|^2 \quad (4)$$

which is positive for even low  $\Delta E_\gamma$  cuts for all values of  $\theta$  (cf Fig. 1). Convoluting this with the resummed ISR structure function for each incoming beam, we obtain a modified  $2 \rightarrow 2$  part of the total cross section which contains all NLO contributions and in addition includes higher order soft and collinear photonic corrections to the Born/one-loop interference. This differs from the standard treatment in the literature (cf eg. [5]) where higher order photon contributions are combined with the Born term only (“Born+”).

The complete result also contains the hard non-collinear  $2 \rightarrow 3$  part convoluted with the ISR structure function:

$$\begin{aligned} \sigma_{\text{res,+}} = & \int^{\Delta(E,\theta)} dx_i d\Gamma_2 f_{\text{ISR}}^{(e^+)}(x_1) f_{\text{ISR}}^{(e^-)}(x_2) |\mathcal{M}_{\text{eff}}^{\text{res}}|^2 \\ & + \int_{\Delta(E,\theta)} dx_i d\Gamma_3 f_{\text{ISR}}^{(e^+)}(x_1) f_{\text{ISR}}^{(e^-)}(x_2) |\mathcal{M}^{2 \rightarrow 3}|^2 \end{aligned} \quad (5)$$

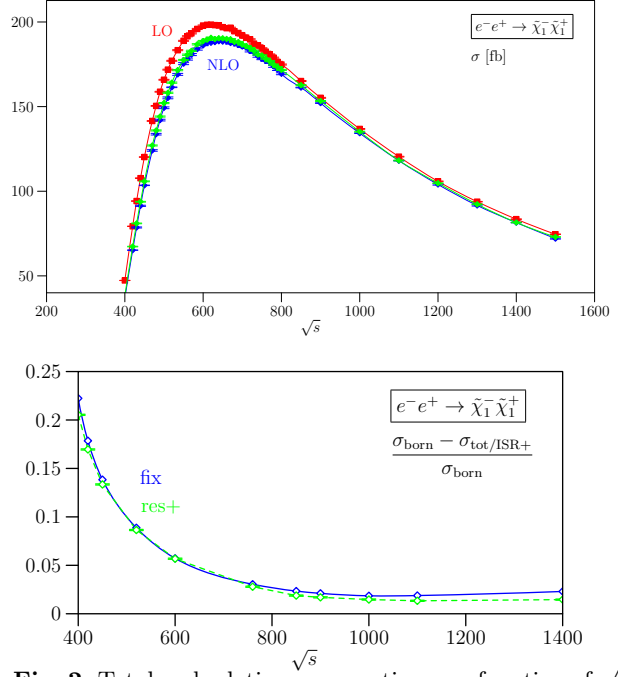


**Fig. 2.** Total and relative cross section as a function of  $\sqrt{s}$ . Upper figure: Born (red, “LO”), fixed order (blue, “NLO”) and fully resummed (green, “NLO”) total cross section, lower figure: relative fixed order (blue, solid) and fully resummed (green, dashed) higher corrections with respect to Born result

The resummation approach eliminates the problem of negative weights (cf. Fig. 1) such that unweighting of generated events and realistic simulation at NLO are now possible in all regions of phase-space.

## 3 Results

### Total cross section and relative corrections

Figure 2 shows the c.m. energy dependence of the total LO and NLO cross section for chargino production for the mSugra point SPS1a’ [3] and the relative corrections with respect to the Born result. The corrections are mostly in the percent regime and can reach 20% in the threshold region.

### Cutoff dependencies

Fig. 3 compares the  $\Delta E_\gamma$  dependence of the numerical results from a semianalytic fixed-order calculation with the Monte-Carlo integration in the fixed-order and in the resummation schemes. The fixed-order Monte-Carlo result agrees with the semianalytic result as long as the cutoff is greater than a few GeV but departs from it for smaller cutoff values because here, in some parts of phase space,  $|\mathcal{M}_{\text{eff}}|^2 < 0$  is set to zero. The semianalytic fixed-order result is not exactly cutoff-independent, but exhibits a slight rise of the calculated cross section with increasing cutoff due to the breakdown of the soft photon approximation. For  $\Delta E_\gamma = 1$  GeV (10 GeV) the shift is

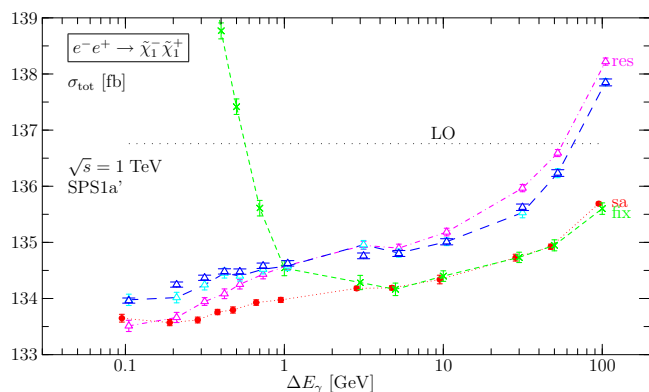


**Fig. 3.** Total cross section dependence on  $\Delta E_\gamma$ : ‘sa’ (red, dotted) = fixed-order semianalytic result; ‘fix’ (green, dashed) = fixed-order Monte-Carlo result; ‘res’ (blue, long-dashed) = ISR-resummed Monte-Carlo result; (magenta, dash-dotted) = same but resummation applied only to the  $2 \rightarrow 2$  part.  $\Delta\theta_\gamma = 1^\circ$ . LO: Born cross section.

about 2 permil (5 permil) of the total cross section. The fully resummed result shows an increase of about 5 permil of the total cross section with respect to the fixed-order result which stays roughly constant until  $\Delta E_\gamma > 10$  GeV. This is due to higher-order photon radiation.

For the dependence on the collinear cutoff  $\Delta\theta_\gamma$ , the main higher-order effect is associated with photon emission angles below  $0.1^\circ$ . For  $\theta_\gamma > 10^\circ$ , the collinear approximation breaks down.

## Event distributions

In Fig. 4 we show the binned distribution of the chargino production angle obtained using a sample of unweighted events. It demonstrates that NLO corrections to the angular distribution are statistically significant and cannot be accounted for by a constant K factor.

Figure 5 shows the difference between the angular event distribution resulting from the fixed order method and the resummation method. As a reference, one standard deviation from the Born event distribution is also given. It is clearly visible that, in the central-to-forward region, even higher order contributions are statistically significant.

## $\sqrt{s}$ dependence of higher order contributions

Figure 6 shows the magnitude of second and higher order photonic effects in different schemes. We compare the fully resummed version (“res+”) to the standard way of adding higher order photonic corrections in the literature (“Born+”), which consists in only convoluting the Born contribution with  $f_{\text{ISR}}$ , and a not completely resummed version (“res”) where higher order photon radiation is taken into account in the  $2 \rightarrow 2$  kinematic regions only. Comparison of “res” and “res+” shows that the additional convolution of

$\mathcal{M}^{2 \rightarrow 3}$  leads to corrections in the percent regime. Comparing “Born+” and “res+”, we see that, for  $\sqrt{s} > 500$  GeV, the additional convolution of the interference term with  $f_{\text{ISR}}$  is equally in the percent regime and additionally changes the sign of the higher order corrections. Therefore, all higher order contributions which are contained in “res+” are significant and have to be taken into account. For more details, cf. [13, 14].

## 4 Conclusions

We have implemented NLO corrections into the event generator WHIZARD for chargino pair-production at the ILC with several approaches for the inclusion of photon radiation. A careful analysis of the dependence on the cuts  $\Delta E_\gamma$ ,  $\Delta\theta$  reveals uncertainties related to higher-order radiation and breakdown of the soft or collinear approximations. To carefully choose the resummation method and cutoffs will be critical for a truly precise analysis of real ILC data. The version of the program resumming photons allows to get rid of negative event weights, accounts for all yet known higher-order effects, allows for cutoffs small enough that soft- and collinear-approximation artefacts are negligible, and explicitly generates photons where they can be resolved experimentally. Corrections for the decays of charginos [15, 16] and non-factorizing corrections are in the line of future work. Equally, a general interface to FormCalc [17] in principle allows for the inclusion of any lepton-collider NLO production process in WHIZARD.

## Acknowledgements

This work was supported by the DFG SFB/TR9 “Computational Particle Physics” and German Helmholtz Association, Grant VH-NG-005.

## References

- W. Kilian, J. Reuter, and T. Robens. *AIP Conf. Proc.*, 903:177–180, 2007.
- Tania Robens. arXiv:0709.1824 [hep-ph].
- J. A. Aguilar-Saavedra et al. *Eur. Phys. J.*, C46:43–60, 2006.
- K. Hagiwara et al. *Phys. Rev.*, D73:055005, 2006.
- T. Fritzsche and W. Hollik. *Nucl. Phys. Proc. Suppl.*, 135:102–106, 2004.
- A. Denner. *Fortschr. Phys.*, 41:307–420, 1993.
- M. Bohm and S. Dittmaier. *Nucl. Phys.*, B409:3–21, 1993.
- Mauro Moretti, Thorsten Ohl, and Jurgen Reuter, 2001. hep-ph/0102195.
- Wolfgang Kilian, Thorsten Ohl, and Jurgen Reuter. 2007. arXiv:0708.4233 [hep-ph].
- R. Kleiss et al. In *Proceedings, Z physics at LEP 1, vol. 3*, Geneva, 1989.
- V. N. Gribov and L. N. Lipatov. *Sov. J. Nucl. Phys.*, 15:675–684, 1972.

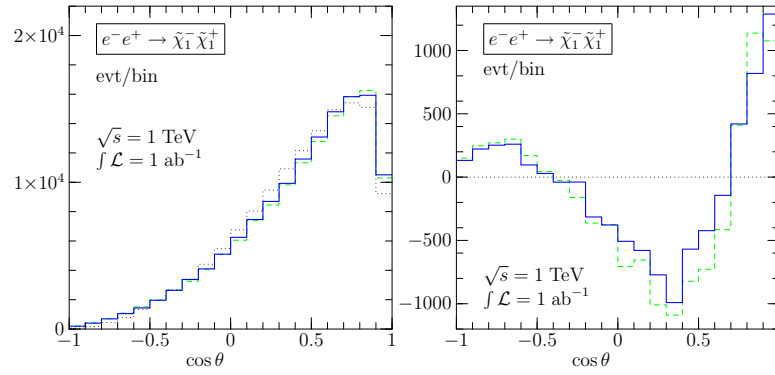


**Fig. 4.** Polar scattering angle distribution for an integrated luminosity of  $1 \text{ ab}^{-1}$  at  $\sqrt{s} = 1 \text{ TeV}$ . Left: total number of events per bin; right: difference w.r.t. the Born distribution. LO (black, dotted) = Born cross section without ISR; fix (green, dashed) = fixed-order approach; res (blue, full) = resummation approach. Cutoffs:  $\Delta E_\gamma = 3 \text{ GeV}$  and  $\Delta\theta_\gamma = 1^\circ$ .

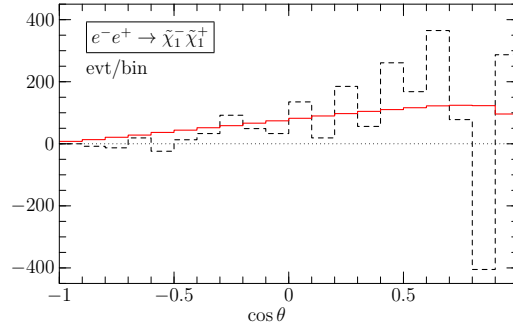


**Fig. 5.** Polar scattering angle dependence of difference between events resulting from completely resummed and fixed order method:  $N_{res} - N_{fix}$ . Standard deviation from Born (red, solid) is shown

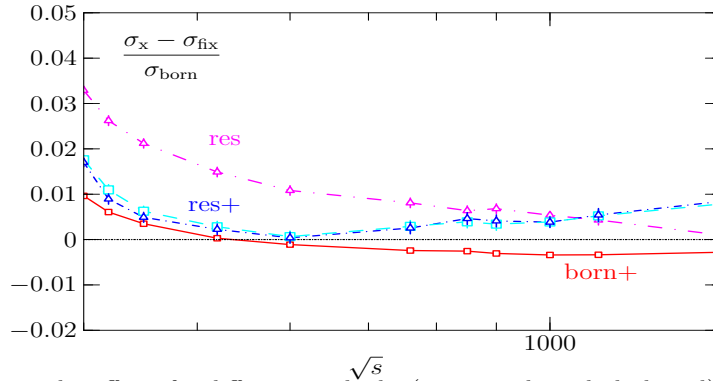


**Fig. 6.** Relative higher-order effects for different methods: (magenta, long dash dotted) =  $\sigma_{res}$ , (blue/ cyan and dash-dotted/ dashed) =  $\sigma_{res+}$ , and (red, solid) =  $\sigma_{Born+}$  vs  $\sigma_{Born}$ .

12. Maciej Skrzypek and Stanislaw Jadach. *Z. Phys.*, C49:577–584, 1991.
13. W. Kilian, J. Reuter, and T. Robens. *Eur. Phys. J.*, C48:389–400, 2006.
14. Tania Robens. PhD thesis, 2006. DESY-THESIS-2006-029, hep-ph/0610401.
15. Krzysztof Rolbiecki. 2007. arXiv:0710.1748 [hep-ph].
16. Junpei Fujimoto et al. *Phys. Rev.*, D75:113002, 2007.
17. T. Hahn and M. Perez-Victoria. *Comput. Phys. Commun.*, 118:153–165, 1999.